CONFIDENTIAL

Copy No. 35

RM No. L8F08

NACA

RESEARCH MEMORANDUM

TRANSONIC DRAG CHARACTERISTICS OF A WING-BODY COMBINATION SHOWING THE EFFECT OF A LARGE WING FILLET

By

Donald C. Cheatham and Max C. Kurbjun

Langley Aeronautical Laboratory
Langley Field, Va.

NATIONAL ADVISORY COMMITTEE
FOR AERONAUTICS

WASHINGTON
September 7, 1948

CONFIDENTIAL

NATIONAL ADVISORY COMMITTEE FOR AERONAUTICS

RESEARCH MEMORANDUM

TRANSONIC DRAG CHARACTERISTICS OF A WING-BODY COMBINATION SHOWING THE EFFECT OF A LARGE WING FILLET

By Donald C. Cheatham and Max C. Kurbjun

SUMMARY

Results of an investigation by the free-fall method are presented herein for a configuration having a body of revolution of fineness ratio 12 and 45° sweptback wing mounted aft of the maximum diameter of the body and faired to the body by fillets. The fillets were designed to provide large increases in the sweep of the leading edge and the line of maximum thickness as the wing root was approached.

Comparison of these results with those for the same configuration without fillets shows that the addition of wing fillets increased the total drag of the configuration by about 35 percent at Mach numbers near 1.0 and about 15 percent at Mach numbers near 1.2. Results indicate that the fillets produced no appreciable change in the wing and tail drags but produced a large increase in body drag due to interference.

INTRODUCTION

The Flight Research Division of the Langley Aeronautical Laboratory is conducting an investigation on a series of wing-body combinations by the free-fall method. The object of this investigation is to determine the transonic drag characteristics of promising transonic and supersonic airplane arrangements. This series has so far been limited to a family of swept wings combined with identical body-tail arrangements.

Previous results by this method and other research have indicated means for reducing the drag of airplane components at transonic speeds. Tests of wing-body combinations are necessary, however, in order to determine whether these results are appreciably altered by interference effects between components. Results of a test of a 45° sweptback wing mounted forward of the maximum diameter of a body of revolution of fineness ratio 12 (reference 1) showed that large interference effects do exist at transonic speeds and, in this case, increase the drags of both wing and body. Results of a further test, reported in reference 2, showed that changing the location of the wing from a position ahead to one behind the body maximum diameter reduced the body drag below that of the body alone but did not appreciably change the drag of the wing.

Preliminary consideration of the flow phenomena about a swept wing at transonic speeds indicated that a large wing fillet fairing the wing to the body and sweeping the line of maximum thickness progressively forward as the wing root was approached might be an effective means for further reducing the drag of the configuration. Results of a test of the wing-body combination, differing only from that of reference 2 in that it had large wing fillets and an airspeed boom, are presented herein as curves showing the variation of drag coefficients with Mach number for the complete configuration and for each of its components. These results in the form of curves showing the variation of drag coefficients with Mach number are compared with the results for the configuration of reference 2 to show the effect of the large wing fillets on the transonic drag characteristics of the configuration.

APPARATUS AND METHOD

Test configuration.- The general arrangement of the configuration is shown in figures 1 and 2 and its details and dimensions are given in figure 3. This wing-body combination differed from that of reference 2 only in that the wing root was faired to the body by means of large wing fillets and in the addition of an airspeed head located on a boom $2\frac{1}{2}$ body diameters ahead of the nose. The details and dimensions of the fillets are shown in figure 4. A description of the airspeed head and the results obtained with it were reported in reference 3. The leading edge of the fillet was a circular arc tangent to the wing at a point 15 inches from the body center line and approximately tangent to the body at the wing root. The trailing edge of the fillet was not faired to the body and had the same sweep as the trailing edge of the outboard part of the wing. The sections of the fillet were faired from the original airfoil section of the wing (NACA 65-009 perpendicular to the leading edge) to an NACA 63-009 section at the root (parallel to the center line of the body). The over-all effect of the fillet on the geometry of the wing, therefore, was to produce a progressive increase in the sweepback of the line of maximum thickness and leading edge as the wing root was approached. The fillets added 17.6 percent to the exposed wing frontal area, 7.3 percent to the total frontal area, and 4.7 percent to the exposed wing plan area. The fillet was an integral part of the wing and faired into rectangular end plates whose surface conformed to the contours of the body. This wing assembly entered the body through rectangular slots and was attached to a force-measuring balance inside the body. A small clearance was allowed between the end plates and the sides of the slots so that the wing was free to move under the restraint of the balance.

Measurements.- Measurement of the desired quantities was accomplished as in previous tests (references 1 and 2) through use of the NACA radio telemetering system and radar and phototheodolite equipment. The following quantities were recorded at two ground stations by the telemetering system:

(1 and 2) The force exerted by the wing on the body and the tail on the tail boom as measured by spring balances.

(3) The retardation or longitudinal acceleration due to drag of the configuration as measured by three sensitive accelerometers covering overlapping ranges.

(4 and 5) The total and static pressures at the airspeed head as measured by multiple aneroid cells. One cell measured the total pressure continuously through the entire range and four cells covered overlapping segments of the same range. The static pressure also had one cell for the entire range with three cells for covering overlapping segments of this range.

Reduction of data.- The velocity of the model in space with respect to a fixed ground point, hereinafter referred to as "ground velocity," was obtained both by a time differentiation of the flight path as recorded by the radar and phototheodolite equipment and by a step-by-step integration of the vector sums of gravitational acceleration and the retardation or longitudinal acceleration due to drag as measured by the accelerometers. True airspeed was obtained by vector summation of ground velocity and horizontal wind velocity at appropriate altitudes.

The total drag was obtained by multiplying the retardation or longitudinal acceleration due to drag a_l (in g units) by the total weight. The drag force on the wing D_W was determined through use of the relation

$$D_W = R_W + W_W a_l$$

where

R_W measured reaction between body and wing in pounds

W_W weight of movable wing assembly in pounds

The drag of the tail fins was obtained from the same relation by using the reaction between the fins and the tail boom and the weight of the movable fin assembly. The body drag was determined by subtracting the drag of the wing and tail from the total.

Values of drag D, static pressure p, and frontal area F were combined to form the nondimensional parameter D/Fp for the complete configuration and each of its components. The Mach number M was determined from the absolute temperature T and the true airspeed. The Mach number was also determined from combinations of the pressure measurements. Values of the conventional drag coefficient based on frontal area C_{D_F} were obtained by use of the relation

$$C_{D_F} = \frac{D/Fp}{\frac{1}{2}\gamma M^2}$$

In the case of the wing and the tail fins, drag coefficients C_D based on the plan area were obtained by multiplying C_{D_F} by the ratio of frontal area to plan area. Where direct comparisons were made between the configuration with fillets and the configurations without fillets, the drag parameters were based on the areas of the configuration without fillets.

The symbols used herein are summarized in the appendix.

RESULTS AND DISCUSSION

A time history of measured and computed quantities obtained from this test is given in figure 5. The variation of ground velocities shown as a solid line is a fairing of the test points computed from the radar and phototheodolite data. The variation of ground velocities shown as a dashed line was computed from the accelerometer data. The agreement between these velocity variations confirms the accuracy of the total drag measurements.

The Mach number variation as computed from the true airspeed (determined from the radar and phototheodolite data) is shown in the time history (fig. 5) and is estimated to be accurate within ±0.01. Four other Mach number variations were determined by all possible combinations of telemeter and atmospheric survey pressure data. These variations show good agreement with the Mach number variations computed from the true-airspeed data. The maximum discrepancy between all Mach number variations obtained was about ±0.02 from an average fairing. The uncertainty in Mach numbers obtained from the telemeter data is believed to be somewhat greater than for the Mach number obtained from the true-airspeed and temperature data. The static and total pressure at the airspeed head was recorded simultaneously over two separate telemeter channels for the first time in the free-fall tests. The two variations of the same quantity were obtained to confirm the accuracy of the measurements. Since the primary purpose of the pressure measurements is to provide an alternate means of obtaining results, which was not needed in this case, telemeter pressure measurements are not presented herein.

The accuracy with which the total drag parameters were determined varied throughout the fall due to the variation in static pressure, and, in the case of the drag coefficients, the accuracy was also affected by Mach number. The uncertainty in the accelerometer measurement is of the order of $\pm0.01g$. This uncertainty is somewhat greater than normal for the equipment and results from impaired reading accuracy due to an undamped electrical oscillation of unknown origin in the telemeter transmitting system. The corresponding uncertainty in the total drag parameter D/F_p is ±0.011 at a Mach number of 0.8 and decreases as the drag and static pressure increases during the free fall to ±0.004 at a Mach number of 1.2. The values of C_{D_F} were somewhat less accurate due to the uncertainty in Mach number of ±0.01. The uncertainty of C_{D_F} is ±0.026 at $M = 0.8$ and ±0.0045 at $M = 1.2$. The wing- and tail-drag measurements show evidence of friction in the balance systems and the presence of this friction is believed to be the cause of the small abrupt changes (see fig. 5) in the measured drag after the major drag rise occurs. It is believed that the peaks of these drag variations represent more nearly the correct values.

The results of this test are presented in figures 6 to 10 as curves showing the variations with Mach number of the parameter D/F_p and drag coefficients for the complete configuration and each component. The variations with Mach number of D/F_p and C_{D_F} for the complete configuration are shown in figure 6. In this figure the drag parameters were based on the areas of the configuration with fillets. The drag per unit frontal area rose from 0.055 of atmospheric pressure at a Mach number of 0.9 to 0.155 at a Mach number of 1.02 and then increased almost linearly to 0.235 at a Mach number of 1.2. The cross hatching in figure 6 shows how the total drag was divided among its components. The wing produced about one-third of the total drag at Mach numbers in excess of unity and the body produced about one-half the drag in the same Mach number range. The remaining drag was contributed by the tail fins.

A comparison of the total drag for the wing-body combinations with and without the wing fillets is given in figure 7 as variations of D/F_p and C_{D_F} with Mach number. For the comparisons made in this and subsequent figures the drag parameters for the configuration with fillets are based on the areas of the configuration without fillets. Figure 7 shows that addition of the wing fillets resulted in an appreciable increase in the total drag of the wing-body combination. The drag rise for the configuration with fillets began at a slightly lower Mach number, increased more slowly at first and then more rapidly than that of the configuration without fillets. The total drag of the configuration with the wing fillets was about 35 percent greater than that without fillets at Mach numbers near 1.0 and about 15 percent greater at Mach numbers near 1.2. If the drag parameters for the configuration with fillets had been based on its own frontal area, the drag parameters of this configuration would be reduced by about 7 percent but would still be larger than that for the configuration without fillets. It is apparent that the fillets produced an unfavorable effect on the transonic drag characteristics of the wing-body combination.

The variations of D/F_p, C_{D_F}, and C_D for the wing with and without fillets are given in figure 8. The drag per unit frontal area of the wing with fillets increased from a value of 0.055 of atmospheric pressure at a Mach number of 0.95 to about 0.13 at $M = 1.02$ and then increased somewhat irregularly to about 0.26 at $M = 1.2$. The irregularities in the drag curves for the wing with fillets are apparently due to the previously discussed friction in the balance system. Since the peaks of the curves of drag coefficient for the wing with fillets correspond closely to the values of drag coefficient for the wing without fillets, it is believed that the addition of the fillets altered the wing drag a negligible amount.

The variation with Mach number of D/F_p and drag coefficients for the tail fins of the two configurations are shown in figure 9. The drag per unit frontal area of the tail of the configuration with fillets increased abruptly from 0.05 of atmospheric pressure at $M = 0.90$ to 0.25 at $M = 0.96$ and then increased erratically to 0.48 at $M = 1.2$. The irregularities of the drag coefficients are again attributed to friction in the balance system. Little difference is indicated, however, in the magnitudes of the tail drag for this configuration and for the configuration without fillets.

The variations of D/F_p and C_{D_F} with Mach number for the bodies of the two configurations are shown in figure 10. In order to present variations of the body drag for the configuration with fillets that are believed to be more nearly correct, the curves of wing and tail drag parameters were faired through the maximum values and the faired values subtracted from the corresponding total drag parameters to give the body drag parameters. At a Mach number of 1.0 the drag of the body of the configuration with fillets was approximately 100 percent greater than that of the body of the configuration without fillets and about 50 percent greater at a Mach number of 1.2. The drag-parameter curves for the body alone (reference 4) are also shown in figure 10 to compare the favorable and unfavorable effects of the two configurations on the body drag. Due to the method of determining the body drag, errors of measurement in wing and tail drag may enter into the body drag. Although the wing- and tail-drag measurements show evidence of friction in the balance system, the results indicate that the addition of the fillets had little effect on the wing and tail drags and the increase in total drag due to the fillets was caused by an interference effect on the body which increased the body drag.

CONCLUDING REMARKS

The drag of a wing-body combination has been measured at transonic velocities by the free-fall method. This configuration consisted of a 45° sweptback wing mounted aft of the maximum diameter of a body of fineness ratio 12 and differed only from a previously tested configuration in that large wing fillets fairing the wing to the body were incorporated.

The results show that fillets of the type employed in this test produced an unfavorable effect on the transonic drag characteristics of the configuration. The drag rise of the configuration with fillets began at a lower Mach number, increasing more slowly at first and then more rapidly than that of the configuration without fillets. The total drag of the configuration with fillets was about 35 percent greater than that without fillets at Mach numbers near 1.0 and about 15 percent greater at Mach numbers near 1.2.

The results also indicate that the addition of the fillets had little effect on the drags of the wing and tail. Therefore, it is evident that the increase in total drag was chiefly due to an interference effect on the body created by the addition of the fillets. At Mach numbers of about 1.0, the drag of the body of the configuration with the fillets was approximately 100 percent greater than that for the body of the configuration without the fillets. This difference decreased to 50 percent greater at Mach numbers near 1.2.

Langley Aeronautical Laboratory
National Advisory Committee for Aeronautics
Langley Field, Va.

APPENDIX

SYMBOLS

g	gravitational acceleration
a_l	longitudinal acceleration in g units
D_w	drag force on the wing
R_w	measured reaction between body and wing in pounds
W_w	weight of movable wing assembly in pounds
D	drag
p	static pressure
F	frontal area
M	Mach number
T	absolute temperature
C_D	conventional drag coefficient
C_{D_F}	conventional drag coefficient based on frontal area
γ	ratio of specific heats (1.4)
D/Fp	drag per unit frontal area per unit static pressure

REFERENCES

1. Mathews, Charles W., and Thompson, Jim Rogers: Free-Fall Measurements at Transonic Velocities of the Drag of a Wing-Body Configuration Consisting of a 45° Swept-Back Wing Mounted Forward of the Maximum Diameter on a Body of Fineness Ratio 12. NACA RM No. L6L26, 1947.

2. Mathews, Charles W., and Thompson, Jim Rogers: Comparison of the Transonic Drag Characteristics of Two Wing-Body Combinations Differing Only in the Location of the 45° Sweptback Wing. NACA RM No. L7I01, 1947.

3. Mathews, C. W., and Thompson, J. R.: Measurements of Static and Total Pressure throughout the Transonic Speed Range as Obtained from an Airspeed Head Mounted on a Freely Falling Body. NACA RM No. L7C04a, 1947.

4. Thompson, Jim Rogers, and Mathews, Charles W.: Total Drag of a Body of Fineness Ratio 12 and Its Stabilizing Tail Surfaces Measured during Free Fall at Transonic Speeds. NACA CB No. L6D08, 1946.

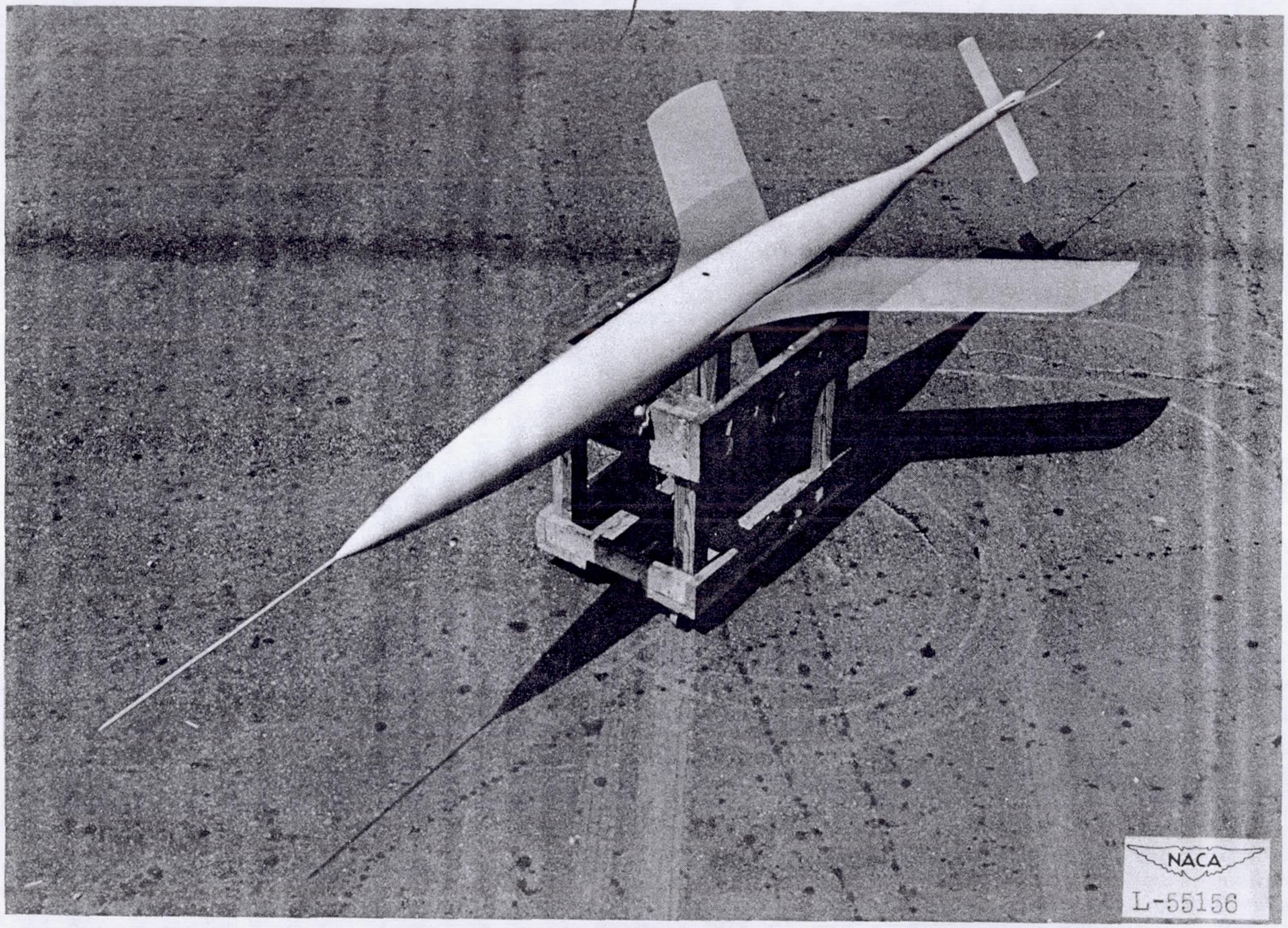

Figure 1.- Three-quarter front view of wing-body combination with wing fillet.

CONFIDENTIAL

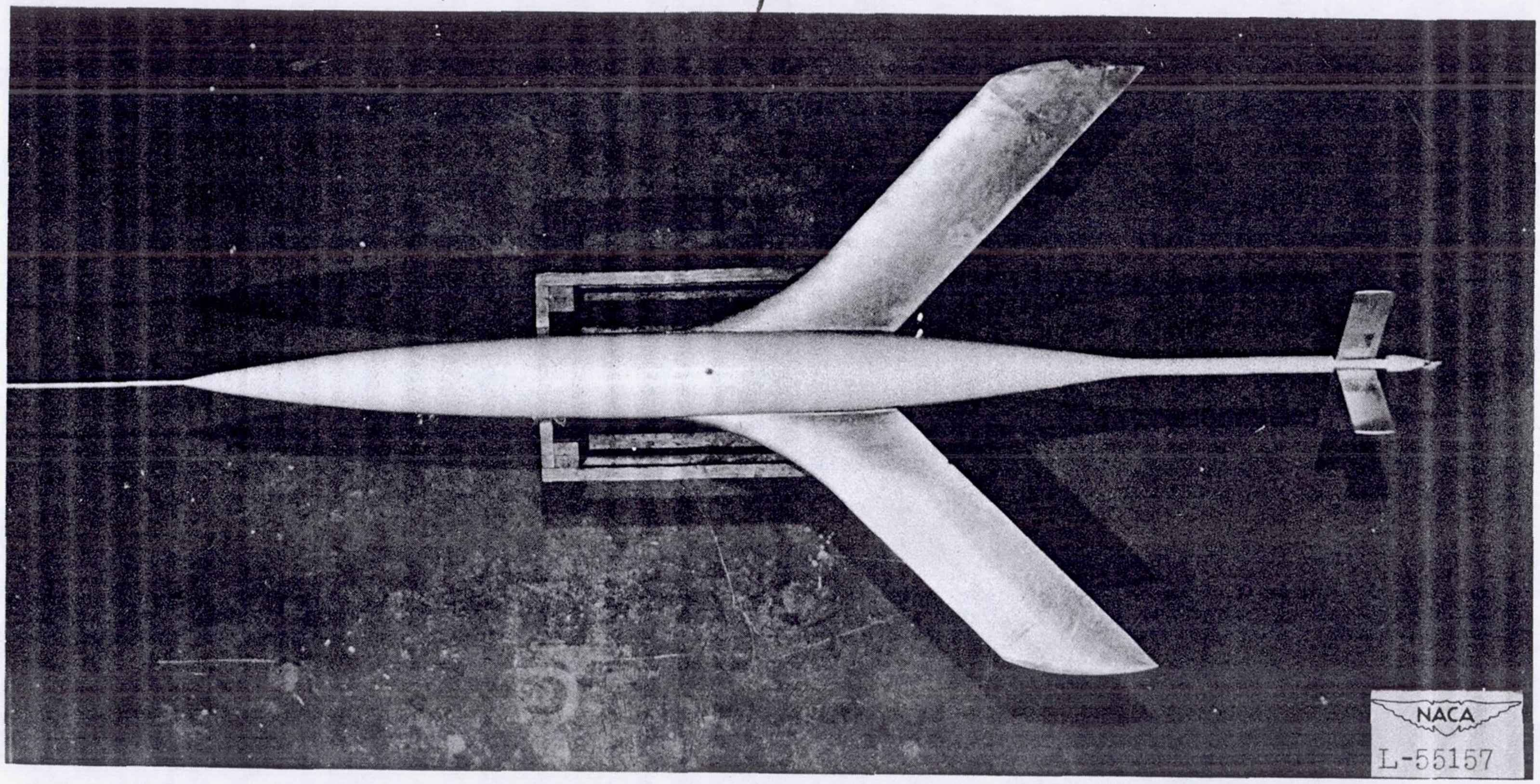

Figure 2.- Top plan view of wing-body combination with wing fillet.

CONFIDENTIAL

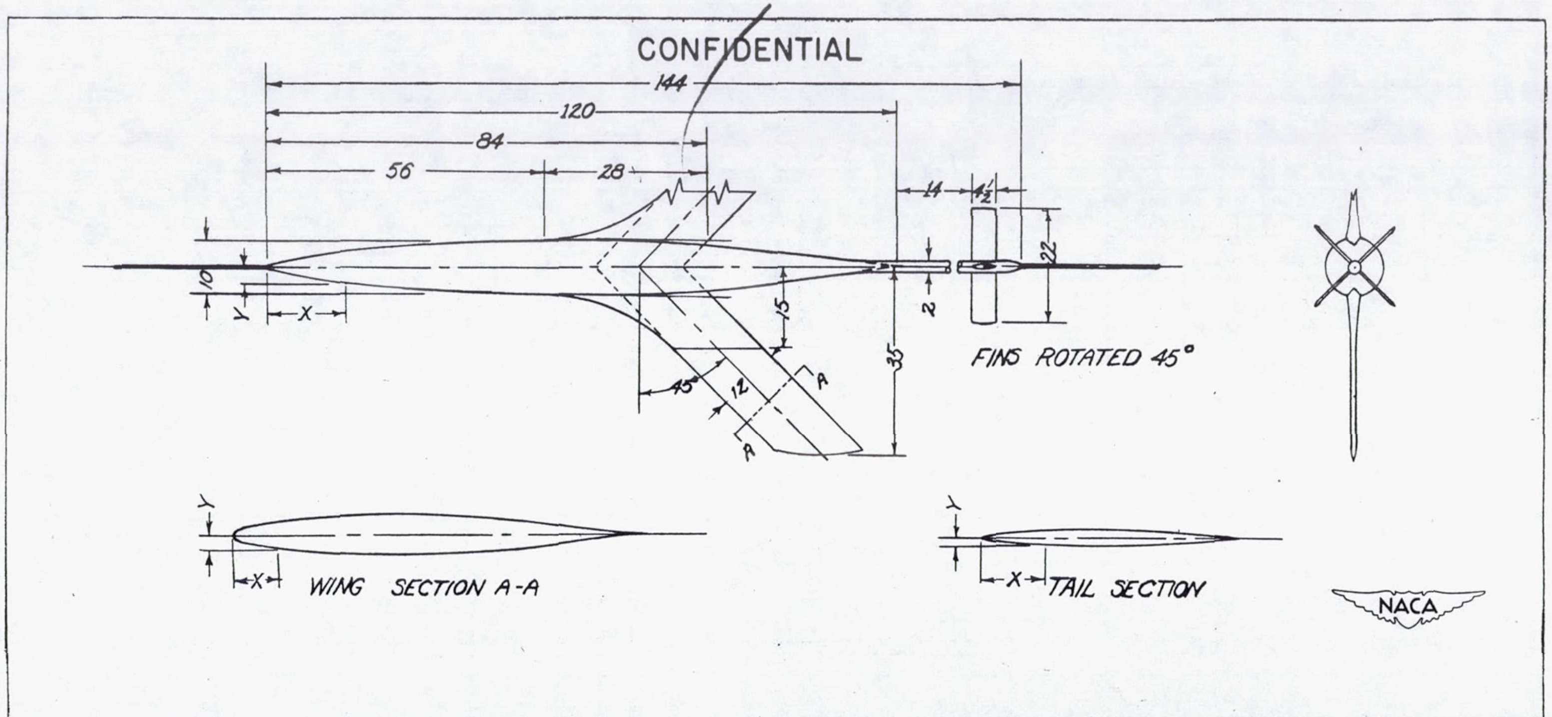

BODY COORDINATES					
X	Y	X	Y	X	Y
0.00	0.000	24.00	3.708	78.00	4.610
.60	.277	30.00	4.158	84.00	4.274
.90	.358	36.00	4.489	90.00	3.754
1.50	.514	42.00	4.719	96.00	3.031
3.00	.866	48.00	4.876	102.00	3.222
6.00	1.446	54.00	4.971	108.00	2.350
9.00	1.936	60.00	5.000	114.00	.526
12.00	2.365	66.00	4.955	120.00	.000
18.00	3.112	72.00	4.828	NOSE RADIUS	0.060

DIMENSIONS - SQ FT	
BODY FRONTAL AREA	0.545
WING FRONTAL AREA	.515
TAIL FRONTAL AREA	.074
WING PLAN AREA	7.250
TAIL PLAN AREA	1.232
TOTAL FRONTAL AREA	1.134
WING AIRFOIL SECTION - NACA 65-009	
TAIL AIRFOIL SECTION - NACA 16-006	

Figure 3.- General arrangement and dimensions of wing-body configuration with wing fillet. All dimensions are in inches. Wing sections measured perpendicular to leading edge.

CONFIDENTIAL

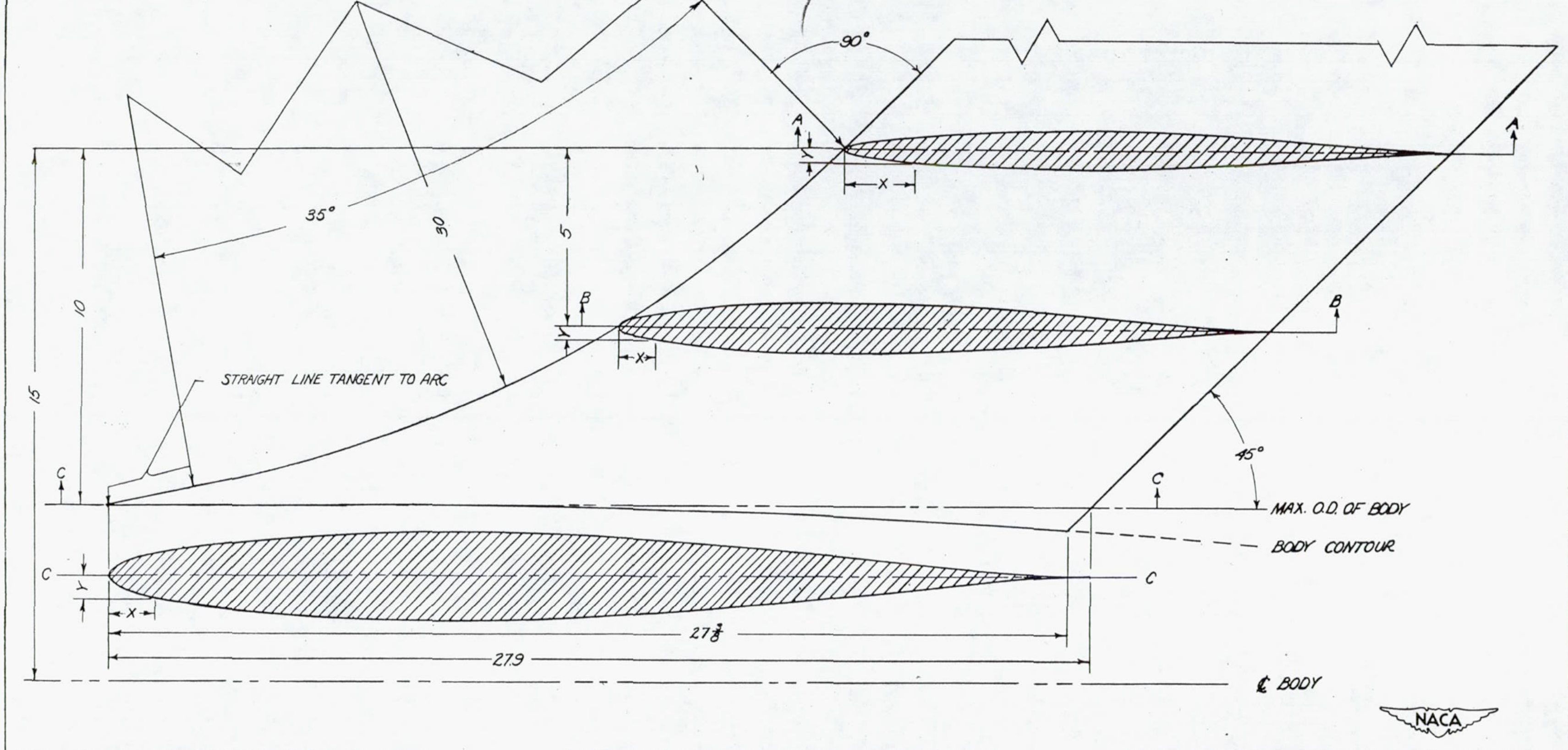

AIRFOIL SECTION A-A

X	Y	X	Y	X	Y
.000	.000	3.495	.447	11.031	.399
.085	.084	4.243	.486	11.880	.343
.127	.101	5.091	.514	12.728	.281
.212	.127	5.940	.532	13.577	.217
.424	.171	6.788	.540	14.424	.151
.849	.235	7.637	.536	15.273	.089
1.273	.286	8.485	.520	16.122	.034
1.697	.328	9.334	.490	16.970	.000
2.546	.396	10.182	.449	L.E. RAD = .098	

AIRFOIL SECTION B-B

X	Y	X	Y	X	Y
.000	.000	3.664	.607	11.908	.484
.092	.114	4.580	.654	12.824	.410
.137	.137	5.496	.684	13.740	.331
.229	.174	6.412	.699	14.656	.251
.458	.237	7.328	.699	15.572	.172
.916	.328	8.244	.682	16.488	.098
1.374	.398	9.160	.652	17.404	.037
1.832	.454	10.076	.606	18.320	.000
2.748	.542	10.992	.550	L.E. RAD. = .108	

AIRFOIL SECTION C-C

X	Y	X	Y	X	Y
.000	.000	5.580	1.115	18.135	.817
.140	.209	6.975	1.193	19.530	.686
.209	.253	8.370	1.239	20.925	.549
.349	.321	9.765	1.256	22.320	.410
.698	.441	11.160	1.241	23.715	.276
1.395	.613	12.555	1.199	25.110	.153
2.093	.741	13.950	1.132	26.505	.055
2.790	.844	15.345	1.043	27.900	.000
4.185	1.002	16.740	.937	L.E. RAD. = .176	

Figure 4.- General arrangement and dimensions of wing fillet. All dimensions are in inches.

CONFIDENTIAL

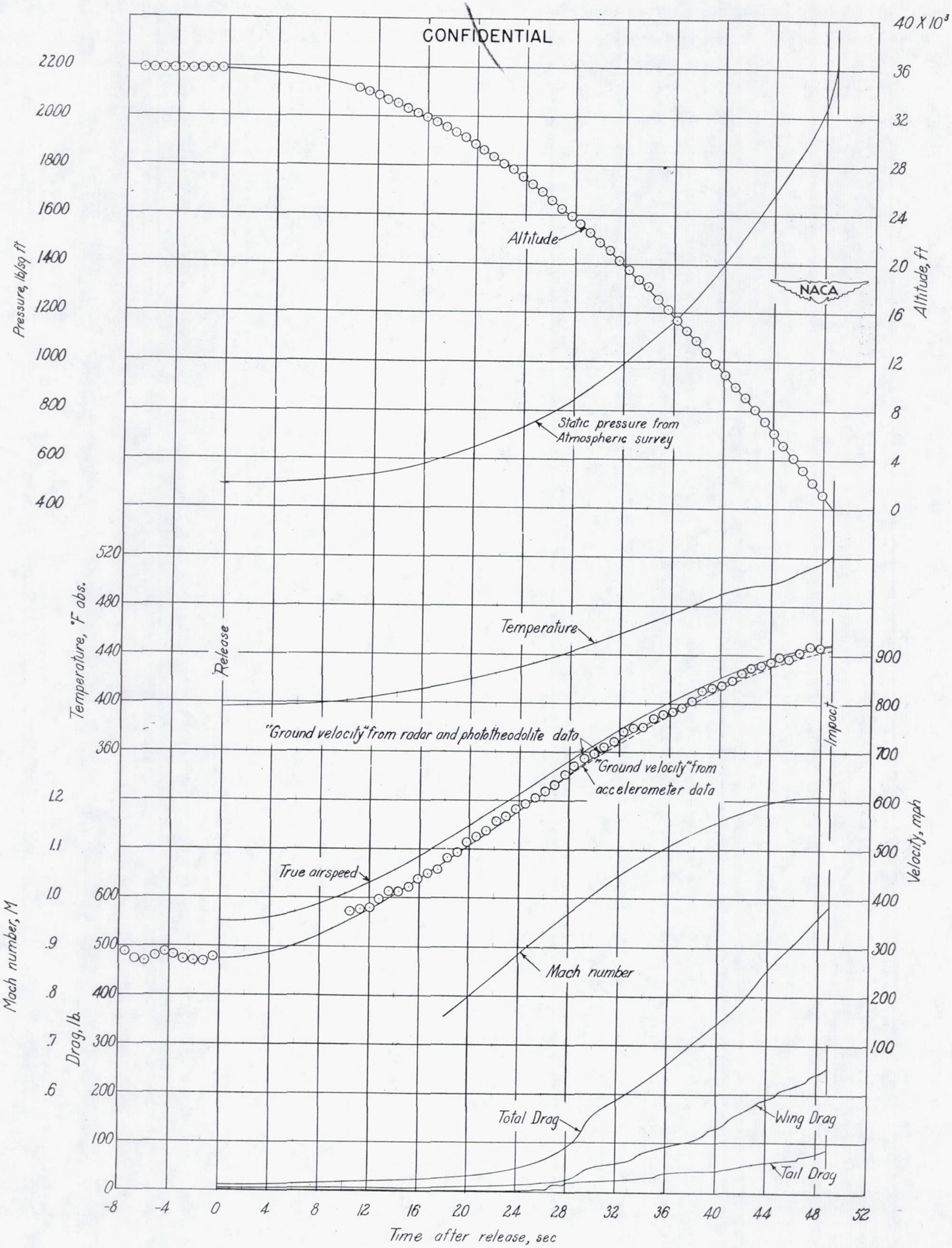

Figure 5.- Time history of free fall of wing-body conbination with wing fillet.

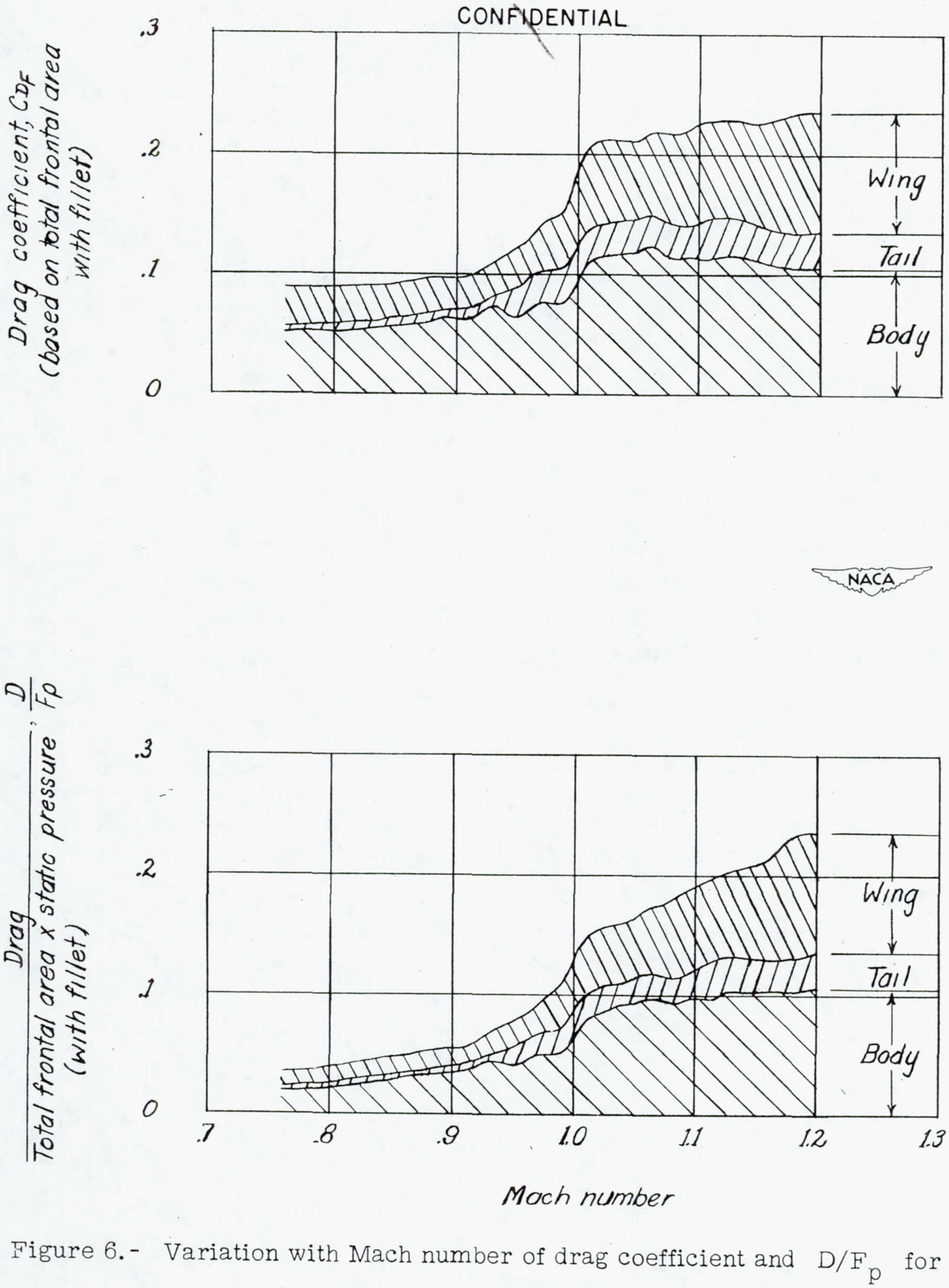

Figure 6.- Variation with Mach number of drag coefficient and D/F_p for the wing-body configuration with wing fillet.

CONFIDENTIAL

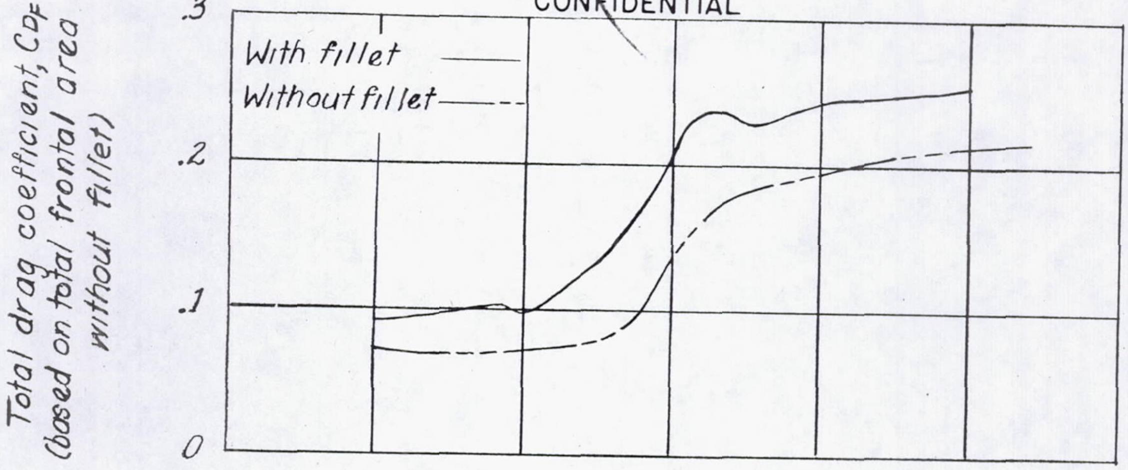

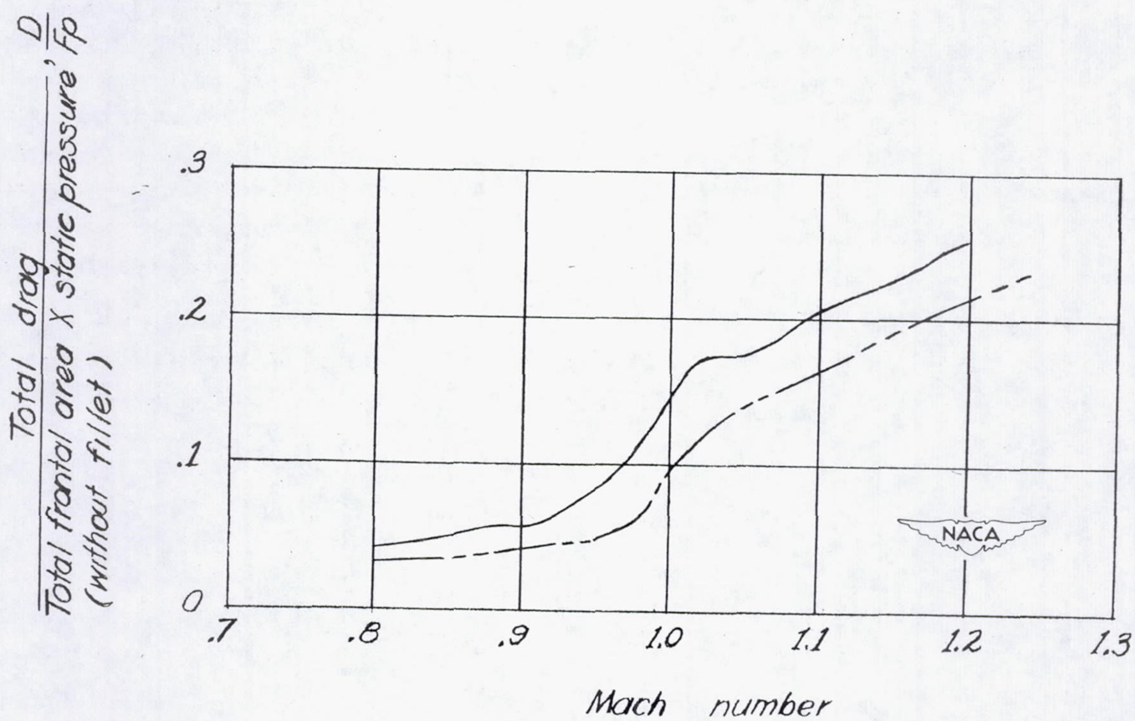

Figure 7.- Comparative variations with Mach number of drag coefficient and D/F_p for the wing-body configuration with wing fillet and without wing fillet.

CONFIDENTIAL

CONFIDENTIAL

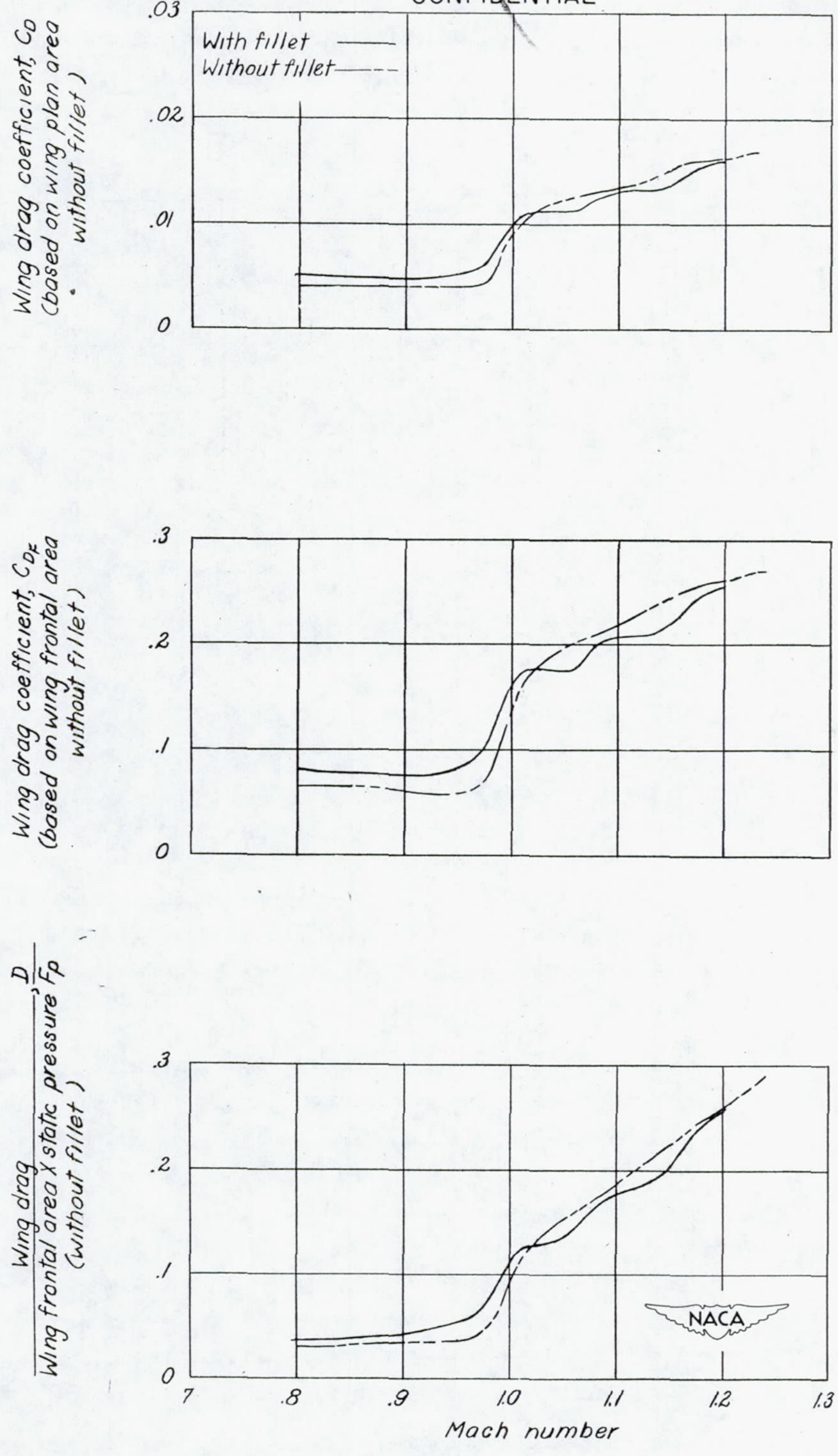

Figure 8.- Comparative variations with Mach numbers of drag coefficients and D/F_p for the wing of the wing-body configuration with wing fillet and without wing fillet.

CONFIDENTIAL

CONFIDENTIAL

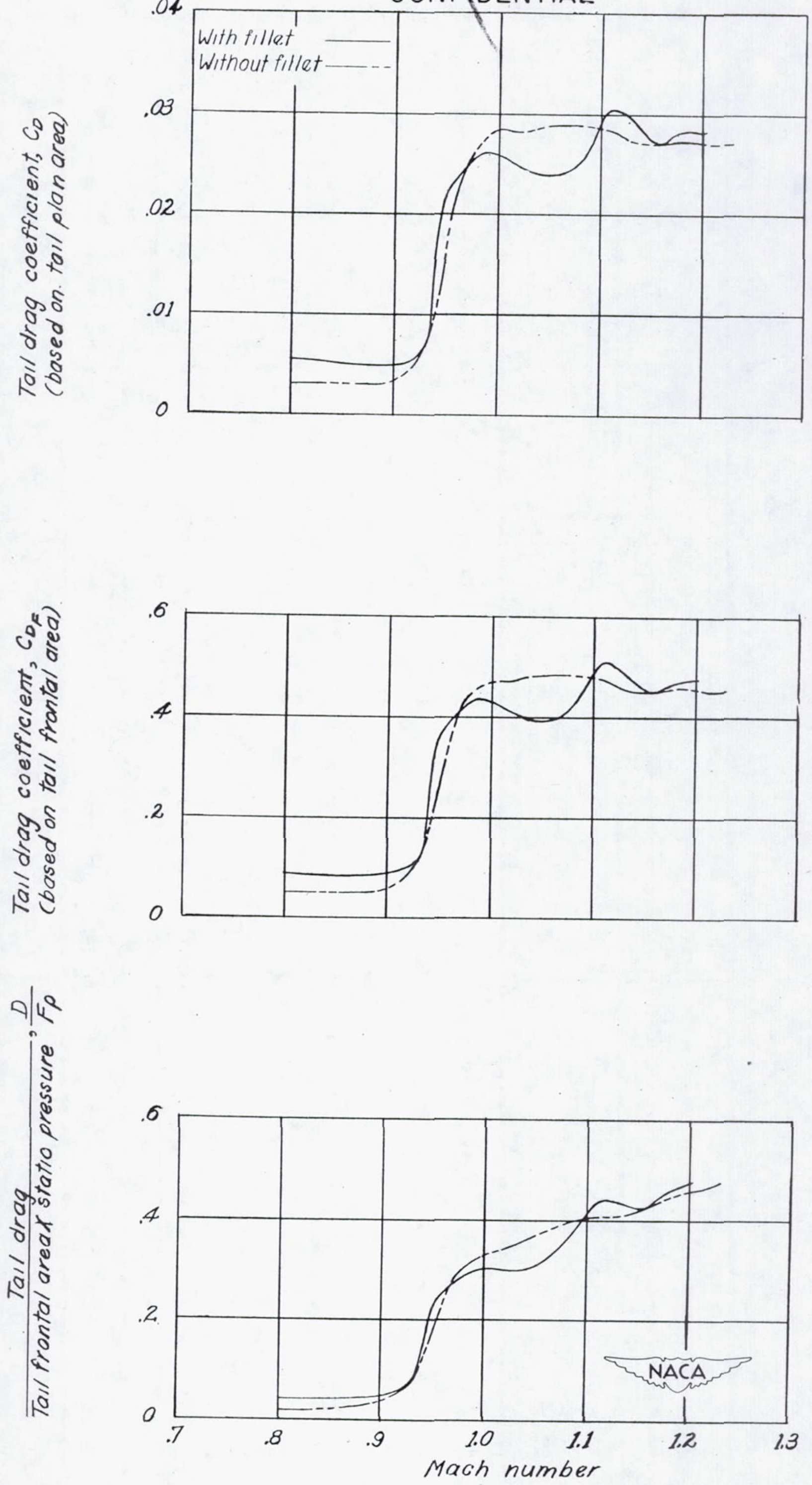

Figure 9.- Comparative variations with Mach number of drag coefficients and D/F_p for the tail fins of the wing-body configuration with wing fillet and without wing fillet.

CONFIDENTIAL

CONFIDENTIAL

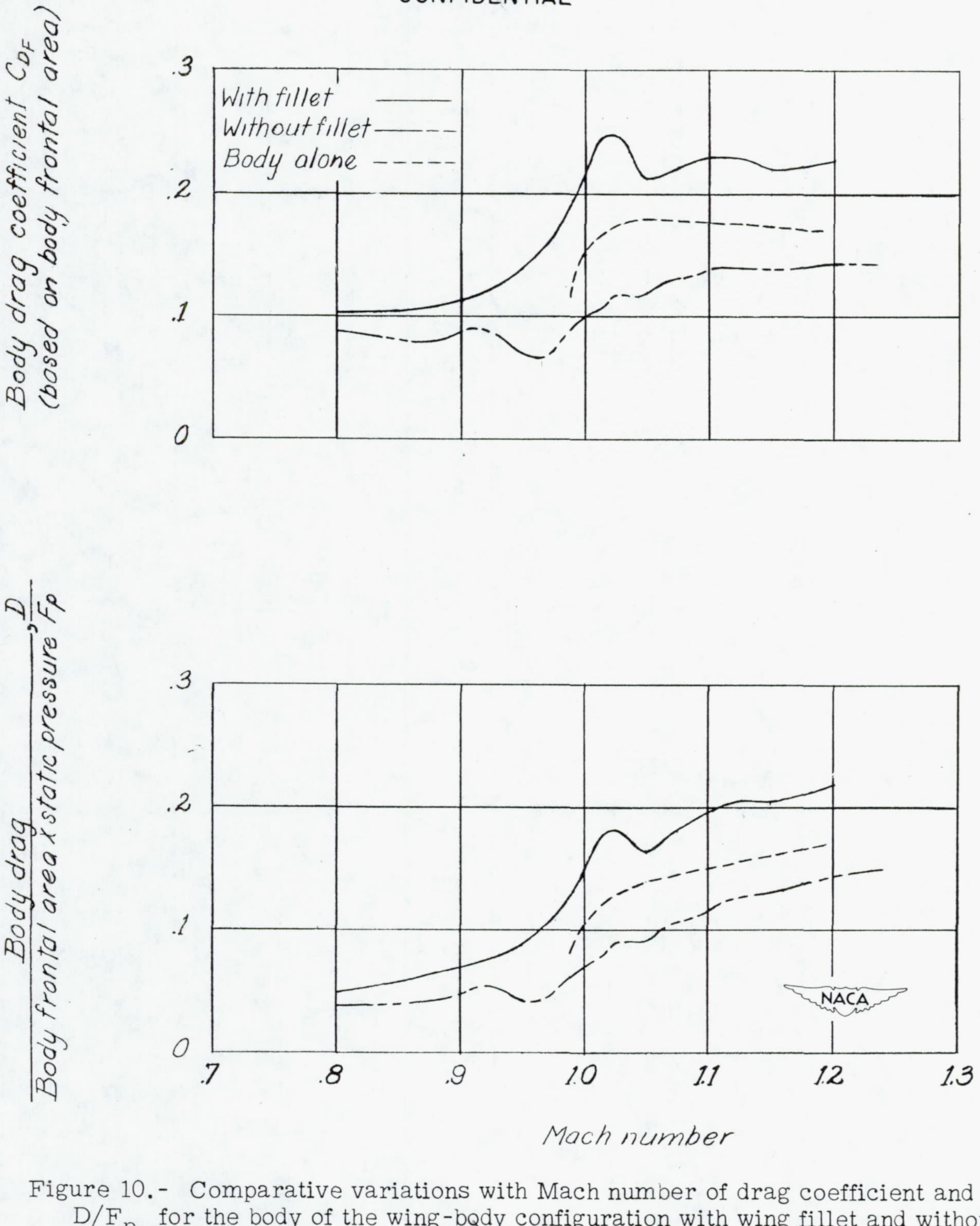

Figure 10.- Comparative variations with Mach number of drag coefficient and D/F_p for the body of the wing-body configuration with wing fillet and without wing fillet.

CONFIDENTIAL